Processes controlling acid attenuation in the unsaturated zone of a Triassic sandstone aquifer (U. K.), in the absence of carbonate minerals

P. DUNCAN MOSS*

Department of Earth Sciences, Leeds University, Leeds LS2 9JT, U.K.

and

W. M. EDMUNDS

British Geological Survey, Crowmarsh Gifford, Wallingford, Oxon OX10 8BB, U.K.

Abstract—Continuous core samples were taken through the unsaturated zone at three sites on the outcrop of Permo-Triassic sandstone in the British West Midlands. Sample sites were chosen for lack of recent, direct anthropogenic disturbance, and for differing vegetation: heathland, birch woodland and conifer forest. Interstitial water was extracted and analyzed for 32 major and trace elements. Solid phases were analyzed for exchangeable cations and mineralogy. The rate of recharge calculated using a Cl mass balance method was three times greater below heathland than below afforested sites owing to higher evapotranspiration rates in the woodlands.

Carbonate minerals were absent from the unsaturated zone at each site. Soil solutions were acidic and soils at the woodland sites were more acidic (pH 4.0) than those at the heathland site (pH 4.5). Acidic interstitial water solutions were found to up to 5.0 m depth in the unsaturated zone and are partially neutralized by two aluminosilicate mineral reactions in the unsaturated zone: cation exchange and K-feldspar dissolution. The rate at which these acid neutralizing reactions act to neutralize acidity is revealed by the rate of depletion of base cations from the unsaturated zone in recharge solutions; K^+ (dissolution), $Ca^{+2} + Mg^{+2}$ (cation exchange). The total base cation depletion rate was greatest below heathland; this can be attributed mainly to the greater rate of SO_4 assimilation by the woodland biome.

INTRODUCTION

IN THE absence of carbonate minerals in the bedrock, acidic surface water and groundwater are neutralized by dissolution reactions and cation exchange reactions involving aluminosilicate minerals (DAHMKE *et al.*, 1986; JOHNSON *et al.*, 1981). Surface waters and groundwaters are more susceptible to acidification if these reactions are: (1) slow in relation to the water flux, or (2) rapid but the total acid neutralizing capacity attributed to these reactions is small.

Surface water is more prone to acidification than groundwater because the residence time of water passing through the soil and shallow bedrock into streams is usually lower than that of water percolating through the unsaturated zone and into deeper groundwater flowpaths. Previous studies have therefore tended to concentrate on the effects of increased acidic deposition on soils and surface water bodies (BRICKER, 1986; CHRISTOPHERSEN *et al.*, 1982; COSBY *et al.*, 1985; GOLDSTEIN *et al.*, 1984; HORNUNG *et al.*, 1986; JOHNSON *et al.*, 1981; NEAL *et al.*, 1986; PAČES, 1986).

In regions where even small quantities of carbonate minerals are present in the bedrock the unsaturated zone and the soil are adequate buffers for preventing acidification of surface waters (BRICKER, 1986) and for neutralizing acidic soil water entering the saturated zone. However, in some regions of the British Isles, slightly acidic groundwater (pH 5.0–6.0) has been recorded at shallow depths coinciding with regions where carbonate minerals are absent from the bedrock mineral assemblage (EDMUNDS and KINNIBURGH, 1986). In acid-impacted regions, high concentrations of certain trace elements in the unsaturated zone and saturated zone may also be a problem for the development of shallow groundwater because of increased mobility of metals in acidic solutions (EDMUNDS *et al.*, 1992). This has highlighted the need for a reappraisal of the silicate mineral reactions that neutralize acidity in the unsaturated zone, and for an assessment of the long term implications of acidic deposition for shallow groundwater in acid-susceptible regions.

GEOLOGICAL SETTING

In Britain the Triassic rocks are subdivided into two groups, the lower mainly arenaceous Sherwood Sandstone Group, and the overlying Mercia Mud-
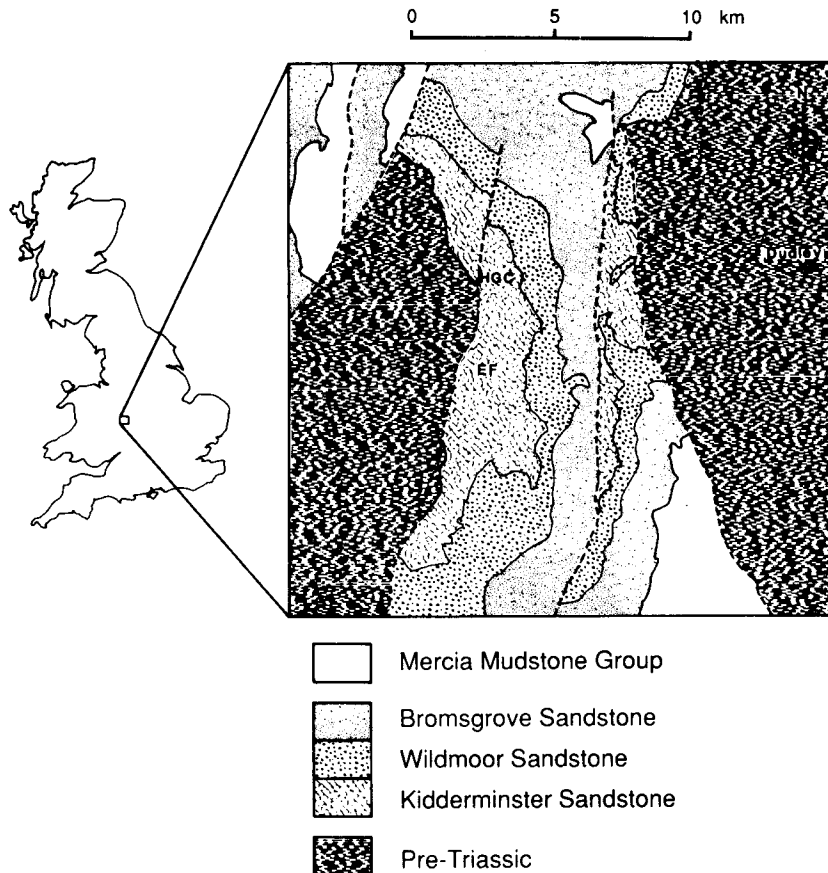
EXHIBIT

68

FIG. 1. Geological sketch map of the Permo-Triassic outcrop in the West Midlands. HGC represents the Highgate Common site and EF the Enville Forest site.

stone Group. The Sherwood Sandstone Group crops out extensively throughout England, and farther north underlies much of the North Sea. The outcrop of the Sherwood Sandstone in the British West Midlands (Fig. 1) has been identified as a region where shallow groundwater is susceptible to acidification (EDMUNDS and KINNIBURGH, 1986). Carbonate minerals are either absent from these units or have been removed by decalcification and slightly acidic groundwater (pH 6.0) has been recorded (KINNIBURGH and EDMUNDS, 1986). The Sherwood Sandstone Group in this region is an important source of water for both domestic and industrial use in the nearby West Midlands conurbation.

For this investigation of the unsaturated zone two sites were chosen for their contrasting land use and for a lack of direct anthropogenic input (such as fertilizers) over their recorded history: (1) Highgate Common—an area of heathland and scrub with some naturally seeded birch woods. This area has been public common land, free of commercial farming practices for at least 40 a and has probably never been subject to intensive cultivation; (2) Enville Forest—a plantation of pine that was seeded on an horse race course in 1949 (37 a before sampling). Both these sites are situated on the Bridgnorth Sandstone, an

aeolian, red-bed sandstone, the basal member of the Kidderminster Sandstone (Fig. 1).

STUDY METHODS

Continuous rock core profiles were taken through the unsaturated zone at Highgate Common (HGC) and Enville Forest (EF), at locations with differing vegetation. Profiles were taken under open heathland (HGC4,5,6 and 7), birch woodland of 20–30 a age (HGC10) and conifer forest of 35–40 a age (EF1 and 2).

The strata below Enville Forest were cohesive and a complete core-sample profile to a depth of 13 m (EF1) was recovered using an air flush, rotary drilling method. The strata below Highgate Common were not cohesive and multiple sample profiles were taken at the heathland site in an effort to optimize drilling methods (Moss, 1989): HGC4 and 5 were drilled using open drive methods, HGC6 was sampled from the face of an open pit and HGC7 was hand augered. The geology and the chemistry of interstitial water in these profiles was repeatable within ±5% and these profiles (HGC4,5,6 and 7) will be referred to as HGC4 for the remainder of the text. The HGC10 and EF2 profiles were also sampled with a hand auger.

Interstitial water was extracted using a heavy-immiscible-liquid displacement technique described by KINNIBURGH and MILES (1983). Each core was subdivided into 20–30 cm sections. One sample was taken from the central part of each section of core, discarding the rim. Approximately 80 g of field-moist rock from each subsample was placed in a

250 ml polypropylene bottle with ~320 g of a heavy immiscible liquid (Arklone, trichloro-trifluoro-ethane) and centrifuged at high speed for 1 h. Interstitial water was then transferred into plastic vials from the surface of the heavy liquid by pipette. Usual recovery rates were 2–4 ml from 80 g of sample (corresponding to 30–60% recovery), however occasional samples with higher clay content released 4–6 ml from 80 g (corresponding to 40–60% recovery). Where possible 5–10 ml of interstitial water was collected from each sample interval by mixing interstitial water extracted from multiple runs of 80 g subsamples.

All interstitial water samples were filtered using a 0.45 μm membrane filter. A 5 ml aliquot was acidified to 1% with HNO_3 and the remaining sample was left unacidified. All samples were kept refrigerated at 4 °C for no more than one week before analysis. The acidified aliquot was analyzed for 27 elements using an ARL 34000C ICP-OES. The unacidified portiion of interstitial water was analyzed colourimetrically for Cl and NO_3–N; for pH using a Radiometer PHM84 pH meter; and for alkalinity by titration. Moisture content of the solid phase was determined by weight loss using ~100 g of sample, placed in an oven at 105 °C overnight.

Modal analysis of the bedrock mineralogy was carried out by point counting grain mounts, and clay minerals were identified by X-ray diffractometry. Whole-rock chemistry was analyzed by X-ray fluorescence. The cation exchange capacity (CEC) of bulk rock samples was determined on Ba-saturated samples by reaction with $MgSO_4$ solution at pH 5.0 ± 0.1 and ionic strength close to that of interstitial water in the unsaturated zone (method modified from RHOADES, 1982; Moss, 1989). Exchangeable cations were determined by displacement with either 0.5 M BaC_2 or 1.0 M ammonium acetate solutions. The exchangeable acidity was determined by alkalimetric titration of aliquots of the 0.5 M $BaCl_2$ extracts (KINNIBURGH, 1986).

RESULTS AND DISCUSSION

Solid phase

The mineralogy of the Bridgnorth Sandstone at each site is almost entirely a mixture of four minerals: quartz (56–79%); K-feldspar (7–17%); and the clay minerals kaolinite and illite. Heavy Fe–Mg minerals are present only in trace quantities, and carbonate minerals and plagioclase feldspar are absent. The sandstone at each site has a fairly uniform mineralogy over the length of each profile, but at the heathland site there are a number of thin (10 cm), laterally discontinuous, clay-rich bands between 1.0 and 2.3 m depth. One 30 cm thick clay-rich band at 2.5 m depth is laterally continuous over the whole HGC sample site. The average cation exchange capacity (CEC) of sandstone was 14 meq/kg, whereas the average CEC of the clay rich bands was 33 meq/kg.

Water flux

Water flux below each vegetation type was calculated using a Cl mass balance method (ALLISON and HUGHES, 1978; EDMUNDS et al., 1988). The Cl mass balance method for calculating recharge was also compared to a water mass balance where the average moisture content was multiplied by an estimate of the

velocity of a tracer peak through the unsaturated zone (Moss, 1989).

Water mass balance. A peak in NO_3–N concentration was observed in a profile through the unsaturated zone of the same lithology as at Highgate Common and below a grassland area (TH1). The leading edge of this peak was at 5.7 m depth and corresponds to the position to which fertilizer (applied 2 a prior to sampling) had moved. This provides an estimate of the average velocity of recharge below this site of 2.8 m/a. By multiplying this value of average recharge velocity by the average moisture content in this profile (120 l/m^3) an estimate of 336 mm/a was obtained for the mean annual recharge under grassland for this climate and lithology.

Chloride mass balance. The rate of recharge for the time represented by a profile interval can be calculated using a Cl mass balance method (EDMUNDS et al., 1988), if the rainfall inputs of Cl and the mean Cl concentration in the interstitial water over a given interval of a profile are known, using the relation:

$$Rd_i = P \cdot Cp/Cs_i \qquad (1)$$

where Rd_i is the mean annual direct recharge (MAR), P is the mean annual precipitation, Cs_i the mean Cl concentration in interstitial water over the profile interval, and Cp the mean concentration of Cl in precipitation including dry deposition. In this study the mean annual precipitation for the catchment is 702 mm (Institute of Hydrology Surface Water Archive) and the value for Cp of 65 μmol/l (2.3 mg/l) for the area was derived from BARRETT et al. (1987). Under steady-state conditions, the Cl concentration below the maximum depth of seasonal recycling of water and solutes (the zero flux plane) should be constant, with only small variations about a mean value due to successive annual inputs.

The length of time (t_d) represented by a profile interval (d) can be calculated from the total Cl in interstitial water over that interval ($Cl_{T,d}$) per square meter:

$$t_d = Cl_{T,d}/Cl_{AN},$$

where

$$C_{T,d} = \Sigma_{n,d} Cs_{i,n} \cdot mc_n \cdot p_{bd} \cdot l_n/1000. \qquad (2)$$

In these expressions Cl_{AN} is the total annual deposition of Cl onto 1 m^2/a, $Cs_{i,n}$ is the concentration of Cl in interstitial water for sample n, mc_n is the moisture content for sample n (g/kg), p_{bd} is the bulk dry density of the formation, l_n is the length of profile represented by subsample n (m), and $\Sigma_{n,d}$ denotes the summation of this expression for n samples in interval d. In this study the total annual deposition of Cl was 45.6 mmol/a and the value for dry bulk density used was 1.5 g/ml.

These methods for calculating recharge and residence time both assume that there is no net assimi-

lation or loss of Cl ions to or from the bedrock, soil or biome and that atmospheric deposition is the only input of Cl. At both sites in this study there was no source of Cl from minerals in the unsaturated zone, and anthropogenic inputs except as a component of atmospheric deposition were absent.

There is evidence that the deposition rate of elements at the land surface can vary between woodland and open heath. REYNOLDS et al., (1989) in comparing the flux of elements in canopy throughfall to the bulk deposition of elements at two upland sites in the British Isles found a 16% increase in the flux of Cl in the canopy throughfall at a woodland site over bulk deposition at a non afforested site. For the present study it was not possible to determine if there had been any enhanced deposition of Cl at the woodland sites compared to the heathland, but it must be assumed that Cl in total deposition is likely to have been higher at woodland areas than at open sites (BARRETT et al., 1987).

The biomass is responsible for the uptake of some Cl on a seasonal basis. For deciduous vegetation much of this Cl will be preferentially concentrated in the leaves (PEREL'MAN, 1977) and returned to the soil as leaf litter. For heathland, including small trees, the storage by vegetation is likely to be negligible but storage of Cl may become significant as the biomass increases. If the upper limit of Cl in dry weight is taken as 0.1% and the biomass dry weight for mature (35 a) forest is 165 t/ha, the Cl uptake would be 2.1 $g/m^2/a$, in this case leading to a storage of ~25% of the deposited Cl. These values must be regarded as order-of-magnitude in the absence of specific data on Cl in the biomass. However it would seem that significant amounts of Cl may be removed from the cycle into storage by trees with the consequence that recharge estimates using Cl must be regarded as minimum values.

Results of recharge calculations

A near steady-state Cl profile was found below the heathland site (HGC4, Fig. 2) and could be used to calculate a recharge rate for this site of 321 mm/a (Table 1). This value compares well to the value obtained for the recharge rate through the same lithology below a nearby grassland site, using the water mass balance method (336 mm/a) employing the nitrate tracer.

Neither of the woodland profiles (HGC10 and EF1) display steady-state recharge conditions (Fig. 2). Both profiles clearly display an upper section with high Cl values above an interval with lower Cl concentrations; recharge rates have been calculated for individual sections of each profile (Table 1). For the HGC10 profile, taken below a deciduous woodland, the recharge for the upper section of the profile (0.0–7.5 m) is 19 mm/a and the residence time is 22.2 a. The lower 1.5 m section of the HGC10 profile is

considered to relate to recharge (104 mm/a) before the woodland developed (some 20–30 a previously) and the upper section represents increased evapotranspiration after afforestation.

For the EF1 profile the residence time represented by the upper section of the profile with high Cl concentrations (0.0–3.5 m) is 12.2 a. This time is considerably less than the apparent age of the afforestation (35 a) and it is possible that this discrepancy is the result of storage of Cl in the biomass as described above or to some site-specific aspect. It therefore remains difficult to assign realistic recharge or residence time estimate for this profile and for the purpose of this study a provisional estimate has been made. Deeper profiles, replicate profiles, further information on biomass accumulation and also more precise site-specific input Cl data are required to estimate recharge beneath forests, although the estimate beneath heathland appears realistic.

WATER–ROCK REACTIONS

Cation exchange

In each profile taken through the unsaturated zone interstitial water is acidic (pH 3.9–6.0; Figs 3–5). In general, the pH of interstitial water increases with depth although the increase in pH is not linear but stepwise. Low pH (p ≤ 4.5) interstitial water occurs in a zone to 2.5 m depth in the Highgate Common heathland profile (HGC4), and to 4.5 m depth (pH = 3.9–4.0) below Enville Forest. Below this zone the pH increases rapidly with depth and is accompanied
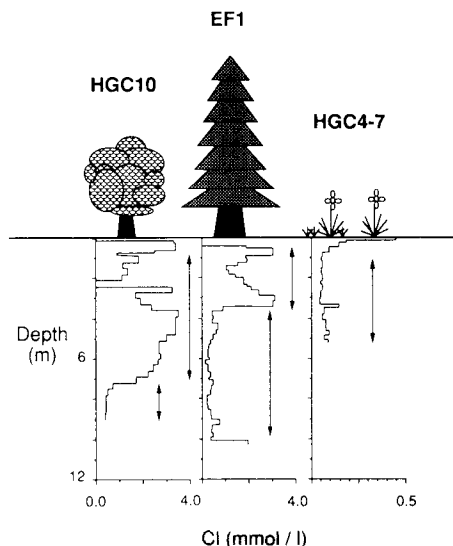

FIG. 2. The concentration of Cl in interstitial water profiles through the unsaturated zone below three types of vegetation. The profiles were taken below natural birch woodland (HGC10), conifer plantation (EF1) and heathland (HGC4-7). The arrows denote the profile intervals used to calculate recharge rates and residence times (see Table 1).

Table 1. Mean annual recharge and average residence time for water calculated using the Cl mass balance method (Eqns 1 and 2 in the text) for sections of the unsaturated zone profiles taken at the sites described in the text (Fig. 2). In the table Rd_i is the mean annual direct recharge (MAR), P is the mean annual precipitation, Cs_i the mean Cl concentration in interstitial water over the profile interval, and Cp the mean concentration of Cl in precipitation including dry deposition

Profile	Depth interval (m)	Residence time (a)	Cs_i (μmol/l)	Rd_i (mm/a)
HGC4	0.5–5.0	1.9	142	321
HGC10	0.5–7.5	22.2	2397	19
HGC10	7.5–9.0	1.0	439	104
EF1	0.5–3.5	12.2	2008	23
EF1	3.5–10.1	4.5	370	123

$Cp = 65 \ \mu$mol/l
$P = 702$ mm/a.

by an increase in the concentration of Ca and Mg in solution relative to the concentration of non-reactive ions Cl or Na (Figs 3–5).

The bulk rock exchange complex in each profile is almost completely saturated with exchangeable Al over the upper zone of low pH interstitial water (Fig. 6). Below this depth the base saturation (exchangeable Ca + Mg) of the bulk exchange complex increases in parallel with the increase in Ca and Mg concentration in the interstitial water profiles (Fig. 6). A reaction front may therefore be identified marking the exchange of base exchangeable cations
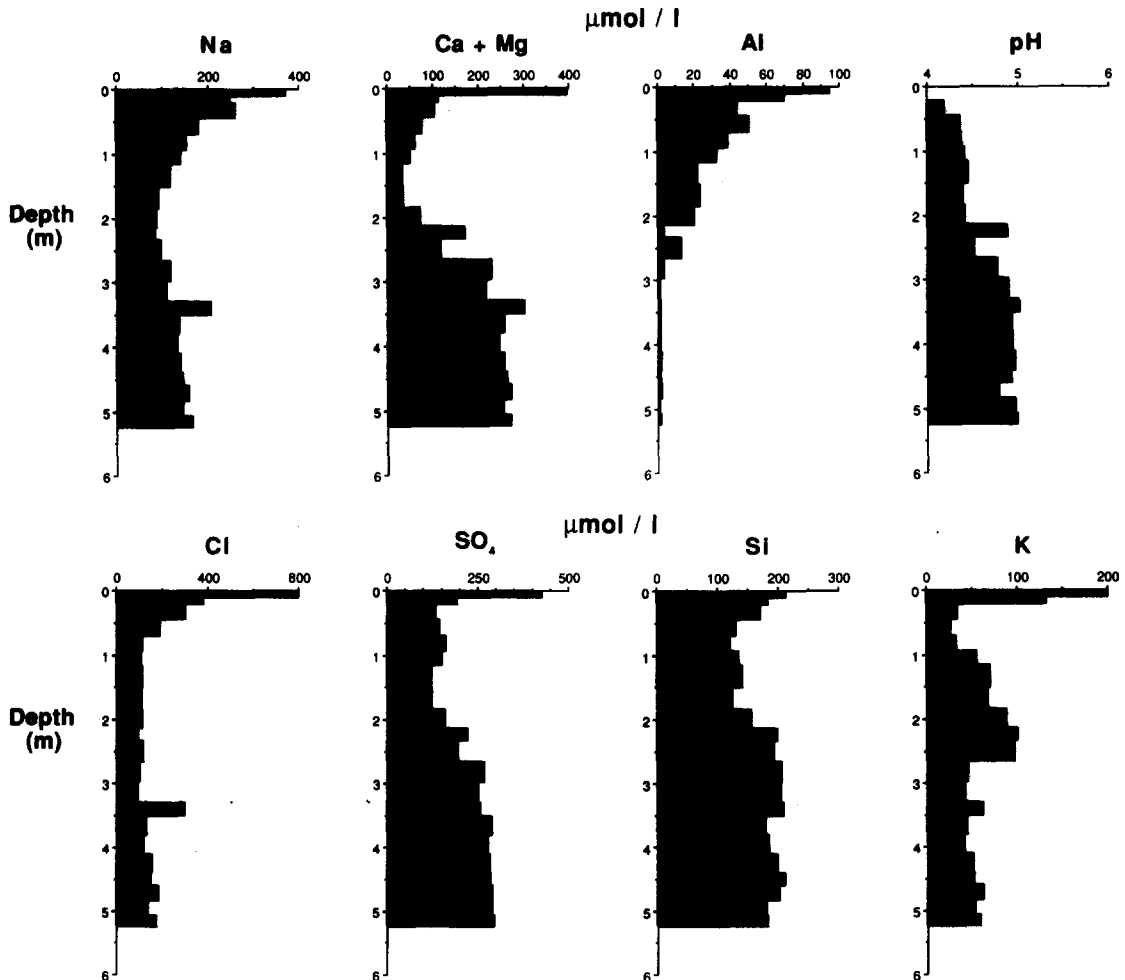

Fig. 3. Interstitial water major element chemistry profiles in the unsaturated zone from below a heathland (HGC4).
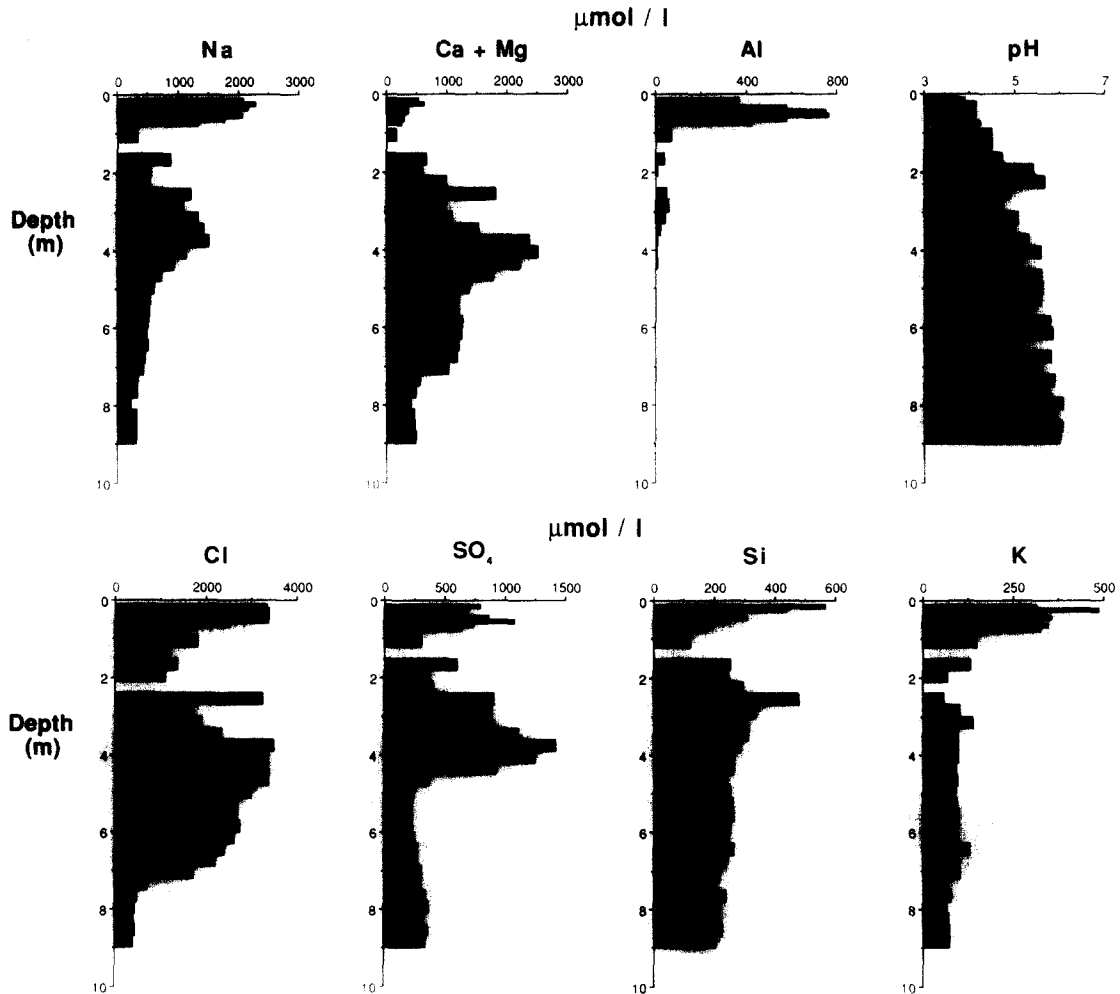
μmol / l

μmol / l

Fig 4. Interstitial water major element chemistry profiles in the unsaturated zone from below a birch woodland (HGC10).

$Ca^{+2} + Mg^{+2}$ for the acid-forming cation Al^{+3} in solution.

$$X\text{-}Ca_3 + 2Al^{3+} \rightleftharpoons X\text{-}Al_2 + 3Ca^{2+}. \qquad (3)$$

The soil acidification model developed by REUSS (1983) was used to simulate the composition of interstitial water in the unsaturated zone in relation to the base saturation of the bulk rock exchange complex. This model considers a simple Al solubility model in conjunction with dissolved Al exchange for Ca adsorbed on the soil exchange complex. The pH and the relative concentrations of Al and Ca in interstitial water in contact with a cation exchange complex of given base saturation can be calculated by this model. Results from the model were compared to the interstitial water chemical analyses from the unsaturated zone profiles, with some minor improvement to the model to allow for SO_4 complexes with dissolved Al (NORDSTROM, 1982). For the purpose of this model Ca and Mg were considered to react in the same way.

The relative concentrations of Al and (Ca + Mg) and pH of interstitial water show close similarity to

the model predictions for given base saturation of the exchange complex (Fig. 7). However, in some cases at high base saturation the relative concentration of (Ca + Mg) is less than that predicted by the model. This can be explained by concentrations of Na in interstitial water samples, which were higher than those in the model.

In some cases the solubility of Al at low base saturation was higher than that predicted by the model. The solubility product of kaolinite was used to describe the solubility of Al because kaolinite is common in the samples from the unsaturated zone. However, kaolinite may not be a valid control for the solubility of Al and previous studies (BACHE, 1974, 1986; JOHNSON et al., 1981; NEAL, 1988) have shown that the apparent solubility of Al in natural waters is difficult to explain in terms of conventional solubility models. The solubility of Al remains a problem in many models of acidification (NEAL, 1989), and kaolinite solubility control is used here as the best fit model for this system.

Cation exchange reactions are rapid, and the

exchange complex in the unsaturated zone can therefore be considered as being in equilibrium with interstitial water. Interstitial water in contact with a cation exchanger of >10–20% base saturation has pH > 5.0 (Fig. 7), and is able to develop positive alkalinity. In this situation the cation content of the ambient solution is dominated by base cations. This implies that while the exchange complex in the unsaturated zone contains sufficient base cations, all acid inputs will be partially neutralized to pH 5.0. The rate at which cation exchange reactions neutralize acidity is governed by maintaining charge balance in interstitial water and therefore the rate at which the reaction progresses is dependant upon the flux of anions (mainly SO_4 and Cl) through the unsaturated zone.

K-feldspar dissolution

In each profile the K/Na ratio in solution is high (mean = 1.05) relative to that of sea water (0.02, GARRELS and CHRIST, 1965), and relative to that in groundwater in the West Midlands Triassic aquifer

(mean = 0.62, EDMUNDS and MORGAN-JONES, 1976). Interstitial water in the heathland profile (HGC4) shows an average steady increase in the concentration of K with depth from 25 μmol/l at 0.5 m to a maximum of 130 μmol/l at 2.5 m depth (Fig. 8). Assuming that K-feldspar dissolution is the only source for K in this section of the profile and that the base of the rooting zone is at 0.5 m and therefore that no K is removed from below this depth by biotic uptake, the increase in K concentration corresponds to a dissolution rate of 10^{-18} μmol/cm^2/s (based on BET surface area measurements and modal analysis of the solid phase). The assumption that K-feldspar is the source for K in solution in this section of the profile is realistic because illite, the only K-bearing mineral in the unsaturated zone, is more likely to be a product of weathering of K-feldspar. In this case precipitation of illite may be a sink for K over some sample intervals and the dissolution rate for K-feldspar calculated here may therefore be a low estimate.

Between 2.3 and 2.7 m depth below the heathland site the concentration of K in interstitial water de-
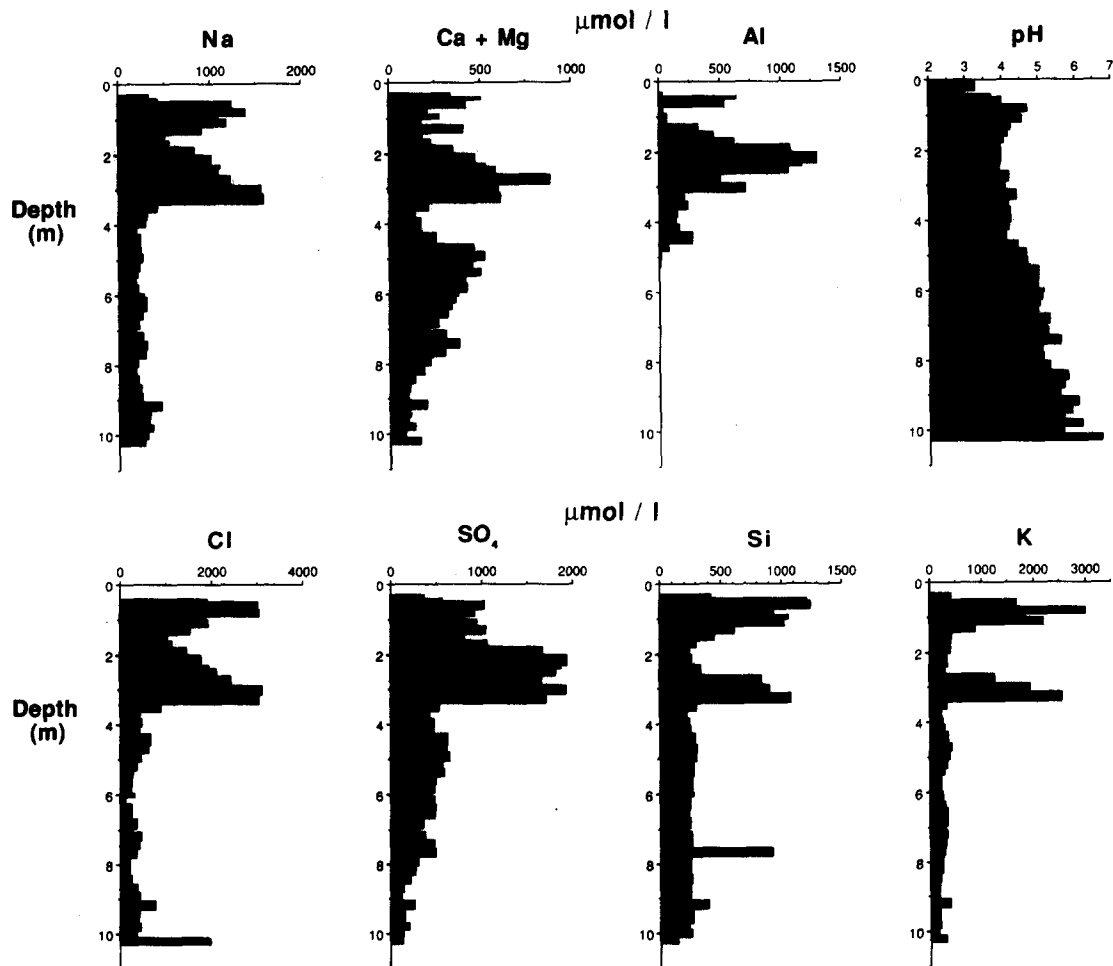

FIG 5. Interstitial water major element chemistry profiles in the unsaturated zone from below a conifer forest (EF1).
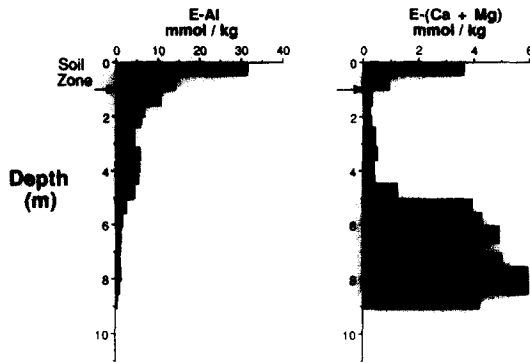
FIG. 6. Exchangeable Al and (Ca + Mg) in the unsaturated zone below Enville Forest (EF1). At 4.5 m depth the exchange complex rapidly changes character from an Al-saturated exchange complex to a (Ca + Mg)-saturated exchange complex. Exchangeable ioins are expressed as mmol/kg bulk sample.

FIG. 8. Concentration of K in interstitial water below the heathland profile. Interstitial water samples from each of the profiles drilled at this site (HGC4,5,6 and 7) are represented here. The average concentration of K increases from $25 \pm 10\,\mu$mol/l at 0.5 m depth to $110 \pm 15\,\mu$mol/l at 2.5 m depth, as shown by the bold line. This increase is attributed to dissolution of K-feldspar. At 2.5 m depth dissolved K is adsorbed to the exchange complex.

creases rapidly (Fig. 8). This decrease in K concentration coincides with increases in pH and (Ca + Mg) concentration and may be the result of exchange of K for (Ca + Mg) adsorbed at mineral surfaces.

Dissolution rates of K-feldspar were experimentally determined in a mixed-flow reactor (Moss,
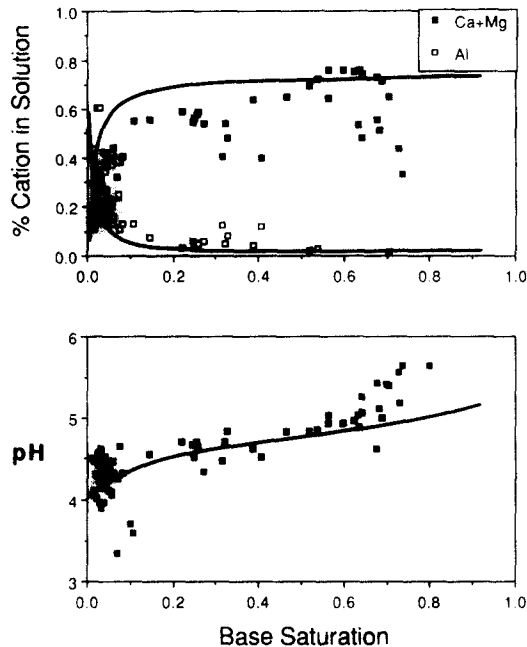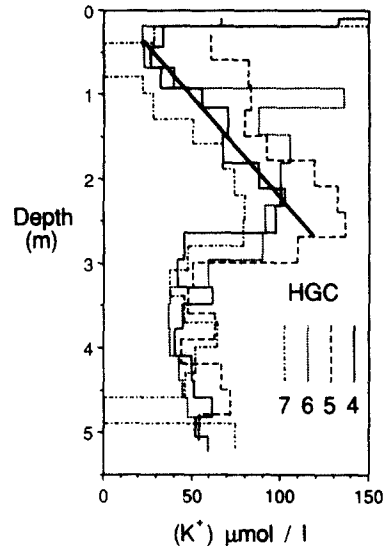

FIG. 7. A comparison of the equilibrium model for cation exchange (after REUSS, 1983) applied to interstitial water chemistry and cation exchange data from unsaturated zone profiles. All samples from this study for which both cation exchange capacity and exchangeable cations were determined are represented on these diagrams and the curves represent the model results. Interstitial water pH and the proportion of the total cation charge equivalents in equilibrium solution accounted for by (Ca + Mg) and Al are plotted as functions of the base saturation of the exchange complex. For each plot 20% of the cation equivalents in solution were assumed to be cations not involved in this exchange reaction (eg. Na).

1989). Freshly crushed K-feldspar and grains hand-picked from samples obtained from the unsaturated zone at Highgate Common were dissolved in separate experiments. For each experiment the input solution was dilute ultrapure HCl and effluent solution pH was measured by an in-line pH meter. Mineral surface area was determined using BET surface adsorption, with N_2 as the adsorbed gas. Dissolution rates were calculated using the concentration of H_4SiO_4 in the effluent solution after the concentrations of reaction products had reached stable values and the solution flow-through rate.

The dissolution rates of fresh crushed grains were $10^{-16.4}$ mol/cm^2/s at pH 4.7 and $10^{-0 16.2}$ mol/cm^2/s at pH 4.2. The dissolution rate of hand-picked grains with naturally weathered surfaces were $10^{-16.9}$ mol/cm^2/s at pH 4.9 and $10^{-16.7}$ mol/cm^2/s at pH 4.2 (Table 2).

The results from the dissolution experiments suggest that feldspar grains with freshly prepared surfaces react only 2–5 times faster to those grains with naturally weathered surfaces under laboratory conditions. However, these hand-picked grains from the unsaturated zone apparently dissolved 10–50 times faster under laboratory conditions than under natural conditions. This discrepancy may be explained as follows:

1. The calculation of the K-feldspar dissolution rate under field conditions assumes that the interstitial water solution is well mixed. This is probably the case on a macro scale but not on a pore-size scale. The dissolution reaction may be proceeding in some

pores but not in others, for example in a dead-end pore where pore solution has been in contact with K-feldspar long enough to have approached equilibrium. The observed dissolution rate is representative of the average rate of dissolution in all pores and may therefore be slower than the actual dissolution rate.

2. Shielding of the grain surfaces by secondary minerals or neighboring minerals may result in poor estimates of the total wetted surface area of feldspar in the unsaturated zone (VELBEL, 1985).

3. High concentrations of dissolved Al in interstitial water may inhibit the dissolution reaction of feldspar (CHOU and WOLLAST, 1985; DREVER and SWOBODA-COLBERG, 1989).

4. Lower ground temperature than that used for the dissolution experiments probably resulted in a faster rate of dissolution in the laboratory (PAČES, 1983; VELBEL, 1990).

There is thus a discrepancy between the dissolution rates of K-feldspar determined in the laboratory, and those determined from field calculations. This highlights the need for care when applying laboratory-derived dissolution rate laws to more realistic field conditions.

MASS BALANCE OF THE UNSATURATED ZONE

Effective acid neutralizing capacity

The acid neutralizing capacity (ANC) of a rock has been defined as the total amount of acid that would be neutralized on complete digestion of the rock by acid (VAN BREEMEN et al., 1983). In this form, ANC values are of little use to models of acidification because a silicate rock rarely dissolves completely in a natural system. For the purpose of this study the definition of ANC is modified slightly and termed the effective ANC (EANC). The EANC is defined here as the sum of the total number of moles of each cation that will be depleted from a given mass of rock under

a given set of environmental conditions. The EANC will therefore depend upon: (1) the total number of moles of depletable base cations per unit mass of rock; (2) the type of cations and the mechanisms by which those cations are depleted; and (3) the pathway of the water through the unsaturated zone. The EANC of any rock mass is therefore partially dependant upon outside influences (soil pH, porosity and permeability in this example).

In this study two reactions relate to the EANC of the unsaturated zone under the conditions described here, cation exchange and K-feldspar dissolution. The EANC that can be attributed to cation exchange reactions is small (36 eq/m^3) relative to that for K-feldspar dissolution (2500 eq/m^3). This has resulted in the upper 3–5 m of the unsaturated zone being almost completely depleted of exchangeable base cations.

Depletion of the EANC

The relative rates at which the two acid neutralizing reactions act in the unsaturated zone profiles studied here can be seen in the depletion rates of base cations from the unsaturated zone represented by each of the profiles. Base cation depletion rates in the unsaturated zone were calculated as the product of the water flux and the average concentration of each cation in interstitial water over the interval used to calculate the water flux (Table 3). In calculating the base cation depletion rates allowance was also made for the flux of cations deposited at the land surface and the calculation was only carried out for recharge below the cation exchange reaction front in each profile.

From the sites studied the output flux of base cations from the unsaturated zone is greatest below the heathland site (1554 eq/ha/a). The flux of cations in the unsaturated zone below the neighboring birch woodland site for the interval representing tree

Table 2. Calculation of K-feldspar dissolution rates. The dissolution rate (r) was calculated as: $r = C_{Si}.f/3.s.m$, where C_{Si} is the steady state concentration of H_4SiO_4 in the effluent solution (mol/l), f is the flow rate (3.7×10^{-6} l/s), s is the mineral surface area (cm^2/g), and m is the mass of K-feldspar (10 g for each run)

Solution pH	$C_{Si} \times 10^{-6}$ mol/l	$r \times 10^{-17}$ mol/cm^2/s	Log(r)
Laboratory crushed K-feldspar; $s = 966 \pm 140$ cm^2/g			
6.7	0.57	7.28	−16.1
6.3	0.29	3.70	−16.4
5.2	0.31	3.96	−16.4
4.7	0.30	3.83	−16.4
4.2	0.54	6.89	−16.2
K-feldspar from the unsaturated zone; $s = 4830 \pm 145$ cm^2/g			
6.2	0.23	0.58	−17.2
4.9	0.48	1.23	−16.9
4.2	0.71	1.82	−16.7
4.0	0.76	1.95	−16.7

Table 3. Estimated cation depletion rates beneath the profiles described in the text. Depletion rate was calculated as the product of the mean ion concentration in interstitial water and the recharge rate (Table 1)

Profile	Depth interval (m)	Concentration (Ca + Mg) K (μmol/l)		Depletion rate (Ca + Mg) K (eq/ha/a)	
HGC4	0.5–5.0	438	46	1406	148
HGC10	0.5–7.5	3262	99	620	19
HGC10	7.5–9.0	918	72	955	75
EF1	0.5–3.5	—	—	—	—
EF1	3.5–10.1	548	259	674	319

growth (639 eq/ha/a) is considerably less than that below the heathland site and less than that for the same profile for the interval representing time before afforestation (1030 eq/ha/a). This can be attributed to more rapid assimilation of SO_4 by trees than by the heathland vegetation, and to the greater water flux through the unsaturated zone below non-forested sites. The flux of cations in recharge water estimated for the EF1 site (993 eq/ha/a) is greater than that below the growing birch woodland and less than that for the heathland, however, in calculating this flux the poorly constrained recharge rate for this site was used. This value for cation flux at EF1 is a minimum value.

The composition of the depleted cations varies between sample sites. Below the Highgate Common (HGC4 and 10) K makes up 3–10% of the depleted base cation charge equivalents whereas below Enville Forest K makes up 32% of the depleted base cation charge. Potassium is derived from the dissolution of K-feldspar. The difference in proportion of K depleted from the unsaturated zone below the EF1 site compared to that from below the HGC sites can be attributed to:

1. Interstitial water with lower pH in the upper section of the EF1 profile (pH 3.5–4.0) compared to that at the HGC sites (pH 4.0–4.5). The dissolution rate of feldspar is pH dependent and lower interstitial water pH in the EF1 profile results in higher rates of dissolution of K-feldspar.

2. Longer residence time for water in the unsaturated zone below the forest site therefore allowing more time for slow mineral dissolution reactions to act.

CONCLUSIONS

At the sites studied in the British West Midlands acidic soil solutions passing downward through the unsaturated zone are neutralized by two reactions involving aluminosilicate minerals, namely cation exchange and K-feldspar dissolution. The factors controlling the relative rates at which two reactions act to reduce acidity of recharge solutions in the unsaturated zone below sites of constrasting vegetation are ultimately dependent upon processes external to the unsaturated zone. These processes mainly concern the interactions of atmospheric deposition with vegetation, and of vegetation with soil solutions:

1. The rate of evapotranspiration at woodland sites is greater than that for grassland sites, and therefore the rate of water recharge below these sites is lower and the residence time for water in the unsaturated zone is greater.

2. The rate at which strong acid anions are assimilated into the biome is greater at woodland sites. This reduces the flux of strong acid anions below woodland sites and this in turn reduces the rate of base cation depletion from the exchange complex in the unsaturated zone.

3. Organic rich woodland soils buffer soil solutions at lower pH than do the heathland soils. Mineral dissolution reactions in these soils will therefore be faster.

The ability of the unsaturated zone to neutralize acidity over a period of time, depends on the effective acid neutralizing capacity (EANC) of the bedrock. The EANC is dependent upon the type of reactions that neutralize acidity and is calculated as the sum of the cations that will be depleted from the bedrock under the present conditions.

Editorial handling: Brian Hitchon.

REFERENCES

ALLISON G. B. and HUGHES M. W. (1978) The use of

environmental chloride and tritium to estimate total recharge to an unconfined aquifer. *Aust. J. Soil. Res.* **16**, 181–195.

BACHE B. W. (1974) Soluble aluminium and calcium–aluminium exchange in relation to the pH of dilute calcium chloride suspensions of acid soils. *J. Soil Sci.* **25**, 320–332.

BACHE B. W. (1986) Aluminium mobilization is soils and waters. *J. geol. Soc. Lond.* **143**, 699–706.

BARRETT C. F., ATKINS D. H. F., CAPE J. N., CRABTREE J., DAVIES T. D., DERWENT R. G., FISHER B. E. A., FOWLER D., KALLAND A. S., MARTIN A., SCRIVEN R. A. and IRWIN J. G. (1987) *Acid Deposition in the United Kingdom* 1981–1985. Warren Spring Laboratory, Stevenage.

VAN BREEMEN N., MULDER J. and DRISCOLL C. T. (1983) Acidification and alkalinization of soils. *Plant and Soil* **75**, 283–308.

BRICKER O. P. (1986) Geochemical investigations of selected Eastern United States watershed affected by acid deposition. *J. geol. Soc. Lond.* **143**, 621–626.

CHOU L. and WOLLAST R. (1985) Steady state kinetics and dissolution mechanisms of albite. *Am. J. Sci.* **285**, 963–993.

CHRISTOPHERSEN N., SEIP H. M. and WRIGHT R. F. (1982) A model for stream water chemistry at Birkenes, Norway. *Water Resour. Res.* **18**, 977–996.

COSBY B. J., HORNBERGER G. M. and GALLOWAY J. N. (1985) Modelling the effects of acid deposition: assessment of a lumped parameter model of soil water and stream water chemistry. *Water Resour. Res.* **21**, 51–63.

DAHMKE A., MATTHESS G., PEKDEGER A., SCHENK D. and SCHULZ H. D. (1986) Near surface geochemical processes in Quaternary sediments. *J. geol. Soc. Lond.* **143**, 667–672.

DREVER J. I. and SWOBODA-COLBERG N. (1989) Mineral weathering rates in acid sensitive catchments: extrapolation of laboratory experiments to the field. In *Water–Rock Interaction*, WRI-6 (ed. D. L. MILES), pp. 211–214. Balkema.

EDMUNDS W. M. and KINNIBURGH D. G. (1986) The susceptibility of U.K. groundwaters to acidic deposition. *J. geol. Soc. Lond.* **143**, 707–720.

EDMUNDS W. M. and MORGAN-JONES M. (1976) Geochemistry of groundwaters in British Triassic sandstones: the Wolverhampton–East Shropshire area. *Q. J. Eng. Geol.* **9**, 73–101.

EDMUNDS W. M., DARLING W. G. and KINNIBURGH D. G. (1988) Solute profiles for recharge estimation in semi-arid and arid terrain. In *Estimation of National Groundwater Recharge* (ed. I. SIMMERS), pp. 139–157. D. Reidel, Dordrecht.

EDMUNDS W. M., KINNIBURGH D. G. and MOSS P. D. (1992) Trace metals in interstitial waters from sandstones: acidic inputs to shallow groundwaters. *Envir. Pollut.* (in press).

GARRELS R. M. and CHRIST C. L. (1965) *Solutions, Minerals and Equilibria*. Freeman, Cooper & Co.

GOLDSTEIN R. A., GHERINI S. A., CHEN C. W., MAK L. and HUDSON R. J. M. (1984) Integrated acidification study (ILWAS): a mechanistic ecosystem analysis. *Phil. Trans. R. Soc. Lond.* **B305**, 409–425.

HORNUNG M., ADAMSON J. K., REYNOLDS B. and STEVENS

P. A. (1986) Influence of mineral weathering and catchment hydrology on drainage water chemistry in three upland sites in England and Wales. *J. geol. Soc. Lond.* **143**, 627–634.

JOHNSON N. M., DRISCOLL C. T., EATON J. S., LIKENS G. E. and McDOWELL W. H. (1981) 'Acid rain', dissolved aluminium and chemical weathering at the Hubbard Brook experimental forest, New Hampshire. *Geochim. cosmochim. Acta* **45**, 1421–1437.

KINNIBURGH D. G. (1986) Towards more detailed methods for quantifying the acid susceptibility of rocks and soils. *J. geol. Soc. Lond.* **143**, 679–690.

KINNIBURGH D. G. and W. M. EDMUNDS (1986) The susceptibility of U. K. groundwaters to acid deposition. Hydrogeol. Rept British Geol. Surv., 86/3.

KINNIBURGH D. G. and MILES D. L. (1983) Extraction and chemical analysis of interstitial water from soils and rocks. *Envir. Sci. Tech.* **17**, 362–368.

MOSS P. D. (1989) Porewater–rock interaction in the unsaturated zone of sandstone aquifers. Ph.D. thesis, University of Leeds, U.K.

NEAL C. (1988) Aluminium solubility relationships in acid waters—a practical example of the need for a radical reappraisal. *J. Hydrol.* **104**, 144–159.

NEAL C. (1989) Aluminium weathering/ion exchange for acid impacted systems: the Achilles heel of predictive models? In *Water–Rock Interaction*, WR16 (ed. D. L. MILES), pp. 515–519. Balkema.

NEAL C., SMITH C. J., WALLS J. and DUNN C. S. (1986) Major, minor, and trace element mobility in the acidic upland forested catchment of the upper River Severn, Mid Wales. *J. geol. Soc. Lond.* **143**, 635–648.

NORDSTROM D. K. (1982) The effect of sulphate on aluminium concentrations in natural waters: some stability relationships in the system Al_2O_3–SO_3–H_2O at 298K. *Geochim. cosmochim. Acta* **46**, 681–692.

PAČES T. (1983) Rate constants of dissolution derived from the measurements of mass balance on hydrological catchments. *Geochim. cosmochim. Acta* **47**, 1855–1863.

PAČES T. (1986) Weathering rates of gneiss and depletion of exchangeable cations in soils under environmental acidification. *J. geol. Soc. Lond.* **143**, 673–677.

PEREL'MAN A. I. (1977) *Geochemistry of Elements in the Supergene Zone*. Keter Publishing House.

REUSS J. O. (1983) Implications of the calcium–aluminium exchange system for the effect of acid precipitation on soils. *J. Envir. Qual.* **12**, 591–595.

REYNOLDS B., CAPE J. N. and PATERSON I. S. (1989) A comparison of element fluxes in throughfall beneath Larch and Sitka Spruce at two contrasting sites in the United Kingdom. *Forestry* **62**, 29–39.

RHOADES J. D. (1982) Cation exchange capacity. In *Methods of Soil Analysis 2: Chemical and Microbiological Properties. Agronomy No.* 9 (ed. A. L. PAGE), pp. 149–158. American Society of Agronomy, Madison.

VELBEL M. A. (1985) Geochemical mass balances and weathering rates in forested watersheds of the southern Blue Ridge. *Am. J. Sci.* **285**, 904–930.

VELBEL M. A. (1990) Influence of temperature and mineral surface characteristics on feldspar weathering rates in natural and artificial systems: a first approximation. *Water Resour. Res.* **26**, 3049–3054.